

On Millimetre-Wave Propagation Characterisation for Human Bodies at 62.4GHz

Charles S. C. Leong¹, Jurgen Richter², Andrew R. Nix¹

¹Centre of Communications Research, University of Bristol
Merchant Venturers Building, Woodland Road, Bristol, BS8 1UB, UK. Charles.Leong@bristol.ac.uk

²School of Electronics, University of Glamorgan
Pontyprid, Cardiff, CF37 1DL, UK.

Abstract

The IEEE has recently formed the 802.15.3c task group (TG3c) to prepare new standards for millimetre-wave wireless personal area networks (WPAN). Channel modelling is one of their main activities. This paper contains detailed measurement results and analysis on the effects of human body interactions in the 60 GHz band. A number of volunteers with body weights ranging from 65 to 110 kg were used to study the effects of human body shadowing in an anechoic chamber. Previously, a number of papers had reported averaged attenuation values for the human body at these frequencies, but none contained detailed measurements performed within an anechoic chamber. The measured data can be used to simulate the effects of various human densities using a 3D ray tracing model. These measurements aid the development of next generation WPAN devices, especially in the worldwide unlicensed 60 GHz band.

1. INTRODUCTION

Due to the inherently high absorption characteristics in the 60 GHz millimetre-wave band, various methods have been suggested to mitigate the problems of human and object shadowing. The performance of a 60 GHz system ultimately depends on four major factors: 1) location of the antenna(s), 2) radiation pattern of the antenna(s), 3) room clutter and 4) the density of people in the room. This paper focuses on the issue of human body shadowing. In the literature there is a large variation in the reported values of human body attenuation in the 60 GHz band; ranging from around 20 dB [1], [2], [3] & [4] up to 35 dB [5]. Variations in the specific measurement environment may explain this large discrepancy.

To eliminate environmental effects, twelve individuals of various weights and sizes volunteered to participate in a study of 60 GHz signal attenuation in an anechoic chamber.

2. MEASUREMENT SETUP

Figure 1 shows the measurement hardware. The measurements were conducted at 62.4 GHz using a narrowband continuous wave (CW) signal. The receiving

hardware uses intermediate frequency (IF) down conversion. The transmitted signal was generated using a phased locked loop (PLL) synthesiser with an enhanced frequency stability of ± 1 kHz. The 20.8 GHz PLL is multiplied by a factor of three, leading to an output frequency of 62.4 GHz.

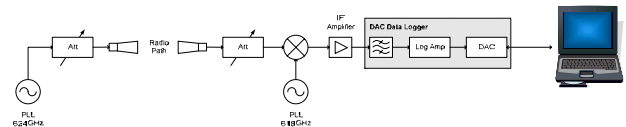


Figure 1: 62.4 GHz Measurement System

At the receiver, the incoming signal is mixed with a 61.8 GHz PLL local oscillator, resulting in a stable IF at 220 MHz. This is then fed into a logarithmic amplifier (Log Amp). The output of the Log Amp is fed into a PCMCIA data acquisition card (DAC). The received signal strength data is stored on a laptop computer for later evaluation.

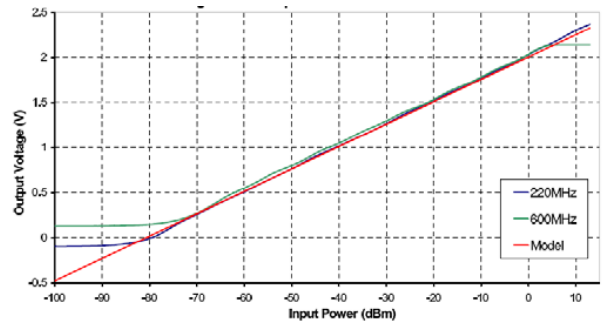


Figure 2: Calibrated Logarithmic Amplifier Curve¹

The performance of a 220MHz and 600MHz Log Amp is shown in Figure 2. In this work only the 220MHz Log Amp was used. As can be seen, the device exhibits a wide linear input response from -80dBm to +13dBm, when compared with the manufacturer's calibration curve. The captured voltages are converted to their corresponding power values in dBm using the expression shown in equation (1).

¹ Courtesy of Telmo R. Fernandes, University of Glamorgan, UK.

$$V[\text{volts}] = 0.02482P[\text{dBm}] + 2.004 \quad (1)$$

V represents the measured voltage from the Log Amp and P is the corresponding power level in dBm.

To measure the attenuation that results from the human body, a 34 dBi lens antenna with a 3 degree half-power beamwidth was used at the transmitter, and a 25 dBi horn antenna with a 9 degree half-power beamwidth was used at the receiver. The high-gain directional lens antenna ensures that accurate measurements can be used through a focused region of the test subject. The high gain antenna also reduces the likelihood of transmitted waves travelling around the side of the body.

Safety precautions include an attenuator at the transmit side to control the maximum output transmit power. A high intensity laser pointer was also used to help align the transmit antenna's boresight on the target area of interest. In order to protect the eyes from accidental exposure to high intensity laser light, a pair of laser protection goggles was worn by all subjects at all times. The laser pointer helped the operator to visually confirm that the transmit antenna was pointing in the intended direction.

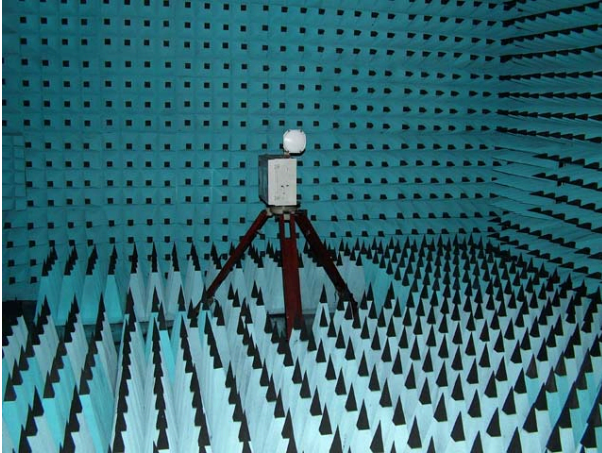


Figure 3: Transmitter Set Up in the Anechoic Chamber

Figure 3 shows the transmit antenna located 4 metres from the subject under test. The Free Space Path Loss (FSPL), P_L , is computed using equation (2).

$$\text{Path Loss, } P_L = 20 \log_{10} \left(\frac{4\pi d}{\lambda} \right) \quad (2)$$

The distance from the transmitter is represented by d , while λ denotes the wavelength (all distances in metres). Using Equation 2 the FSPL at a distance of 4 m (corresponding to the location of the test subject) is 80.40 dB. Each test subject stood 1m in front of the receiver. The total transmit-receive separation distance was 5m. Several layers of Radar Absorbing Material (RAM) were placed on both sides on the receiving antenna to minimise unwanted rays around the sides

of the body. This latter precaution (together with the highly directional transmit antenna) is important since we aim to measure the attenuation of the direct wave passing through the body.

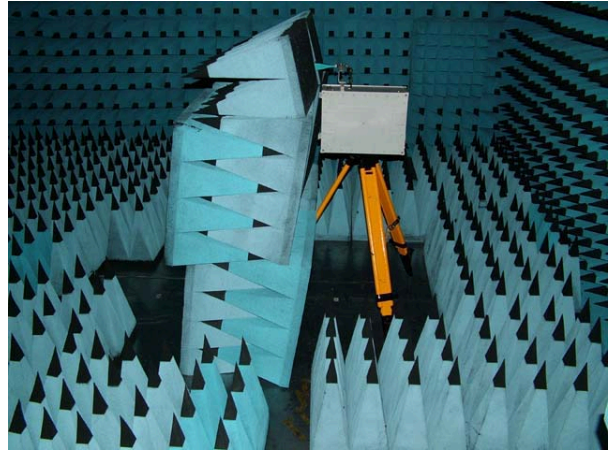


Figure 4: Receiver Set Up in the Anechoic Chamber

A. Safety

The above configuration ensured that the experiment complies with worldwide radio safety regulations. Table 1 depicts the safety limits defined for operation in the US, UK and Japan.

TABLE 1: RF SAFETY REGULATIONS IN THE US, UK, AND JAPAN

Maximum Permissible Exposure (MPE) Average Continuous Exposure Time for 6 minutes			
	FCC	UK	Japan
Power Density, S (mW/cm ²)	5	5	1
Electric Field Strength, E (V/m)	137.3	137.3	61.4
Magnetic Field Strength, H (A/m)	0.364	0.364	0.163

The power density, S , the electric field strength, E , and the magnetic field strength, H , can be computed as shown below

$$\text{Power Density, } S = \frac{P_t(\text{mW}) G_t}{4\pi d^2(\text{cm}^2)} \quad (3)$$

$$S = \frac{E^2}{3770} = 37.7 H^2 \quad (4)$$

P_t represents the transmit power in mW, G_t is the transmit antenna gain (relative to an isotropic source), and d is the distance between the radio exposed subject and the transmitter.

Using equations (3) and (4) we can deduce the exposure levels for S , E , and H for the subject under test. A transmit

power P_t of -4 dBm (0.4 mW) was used at the input to the lens antenna and a distance of 4 m the levels of S , E and H are $0.5 \mu\text{W}/\text{cm}^2$, $1.37 \text{ V}/\text{m}$ and $3.6 \times 10^{-3} \text{ A}/\text{m}$ respectively. These values are many orders of magnitude below the maximum levels defined in table 1.

3. MEASUREMENT PROCEDURES

Figures 5 and 6 show the experimental set up for measuring the impact of the human body attenuation at millimetre-wave frequencies. The transmitter and receiver are separated by a distance of 5m, and the person under test was placed 4m from the transmitter. Measurements were confined to attenuation through the torso. The first phase of measurement saw the subject move from left to right as shown in Figure 5. Measurement snapshots were taken at 5 displacements. The second phase involved 5 measurement snapshots for a range of vertical displacements, as shown in Figure 6. The total experimental exposure time was around one minute for each phase. The exposure time for each measurement point (snapshot) was limited to no more than 10 seconds. For both directions, the separation distance between displacements was 5 cm. A total of 10 measurements were taken for each subject.

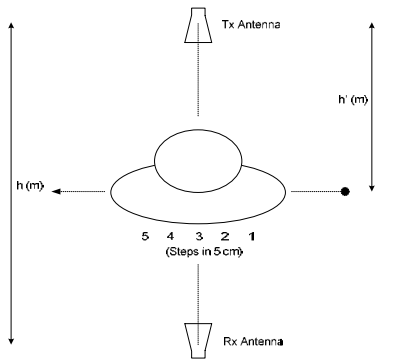


Figure 5: Top View: Left-to-Right Torso Measurement in anechoic chamber

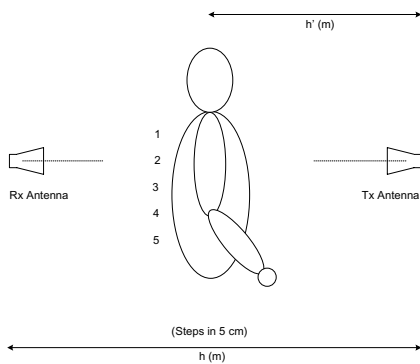


Figure 6: Side View: Top-to-Bottom Torso Measurement in anechoic chamber

4. RESULTS AND ANALYSIS

Figures 7 and 8 show the individual and averaged results for the measurements defined in section 3 for the twelve volunteers.

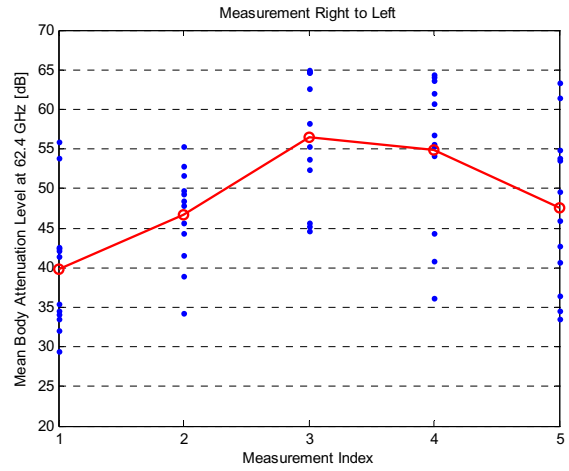


Figure 7: Left-to-Right Torso with mean, $\mu = 48.74 \text{ dB}$ and standard deviation, $\delta = 6.68 \text{ dB}$

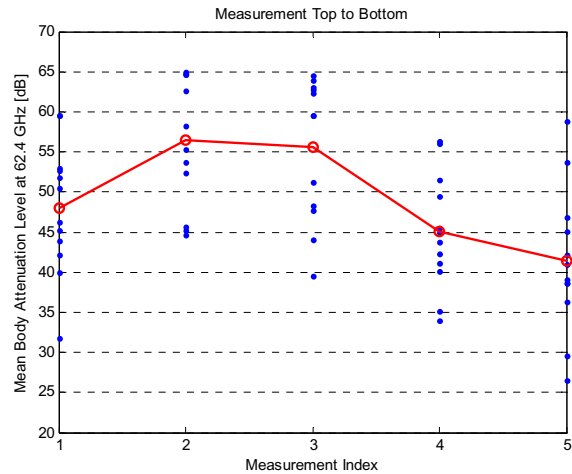


Figure 8: Top-to-Bottom Torso with mean, $\mu = 48.96 \text{ dB}$ and standard deviation, $\delta = 6.69 \text{ dB}$

The results show increases in attenuation beyond the centre point on the torso. From left to right, the mean attenuation is 48.74 dB, with a standard deviation of 6.68 dB. From top to bottom, the mean attenuation is 48.96 dB, with a standard deviation of 6.69 dB.

The large variance between the twelve individuals can be attributed to a number of factors. These include movement during the measurements, differences in physical attributes, and errors in locating the same measurement point for each

individual. The impact of each person’s physical attributes was thought to have the largest impact (this is studied in more detail in the remainder of this section).

The objective of this campaign was not to characterise detailed attenuation values for a given individual, but to determine the range of values that can be expected versus body type, and to determine the overall trend in microwave attenuation level through the torso.

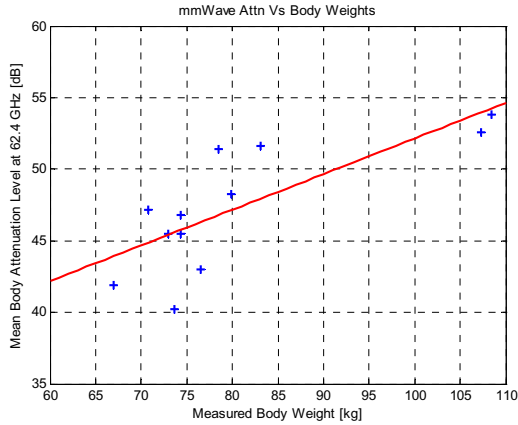


Figure 9: Millimetre-wave Attenuation Versus Human Body Weight

Figures 9 and 10 demonstrate that the observed levels of millimetric attenuation have a high correlation with body weight, and in particular body water content. This is due to the fact that at these frequencies, water absorption is extremely significant. Each point on the curve represents a mean attenuation value taken from the 120 measurements performed for each individual. A body scan weighing machine² was used to approximate the amount of body fat and body water content.

It can be seen from figure 10 that the attenuation can vary by as much as 8 dB between individuals with similar weights (74 kg in this case). This difference can be partly explained by the different levels of body water content at the time of measurement. Variations will also occur as a result of differing muscle and fat compositions.

From the reported measurements data, at 62.4GHz the following relationship between torso attenuation and body weight was derived.

$$\alpha[dB] = 0.24899 \gamma[kg] + 27.256 \quad (5)$$

where α and γ represent the attenuation in dB and the body weight in kg respectively. The relationship between attenuation and body water content is:

$$\alpha[dB] = 1.0671 \beta[kg] + 1.554 \quad (6)$$

where α and β represent the attenuation in dB at 62.4GHz and the water content level (measured in kg) respectively.

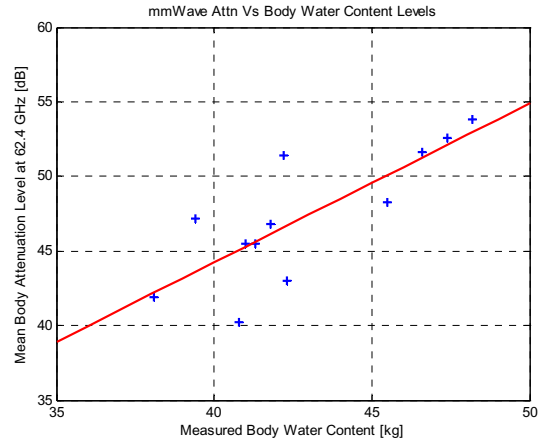


Figure 10: Millimetre-wave Attenuation Versus Human Body Water Content

Figure 11 shows the relationship between the attenuation level and the degree of body fat. The data is clustered over a body fat range of 12 to 20 kg. Most volunteers had a similar level of body fat (15 ± 3 kg, which represents around 20% of their total body weight).

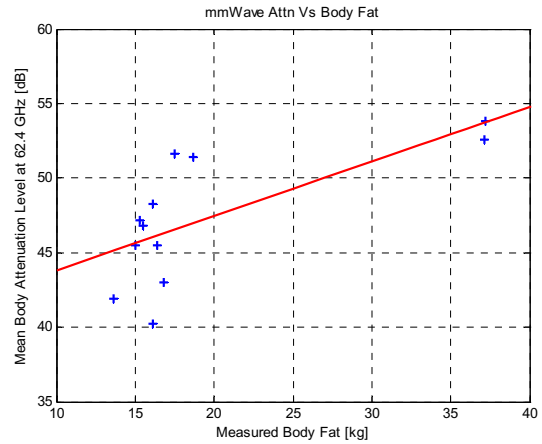


Figure 11: Millimetre-wave Attenuation Versus Human Body Fat

A pseudo deterministic method [6] can now be used to determine the received power level in an environment with a number of obstructions between the transmitter and receiver. This equation can now be used to include the influence of human body shadowing.

² Brand name: B&Q, Model: Pure

$$P_r(d) = P_t + G_t + G_r - 20 \log_{10} \left(\frac{4\pi d}{\lambda} \right) - \sum_{i=1}^N a_i X_i \quad (7)$$

Where $P_r(d)$ represents the received power in dBm at a distance d in meters from the transmitter, P_t is the transmit power to the antenna port in dBm and G_t and G_r is the transmit and receive antenna gain respectively. a_i and X_i are the number and attenuation level for the i^{th} human obstruction intersected by the radio path between the transmitter and the receiver.

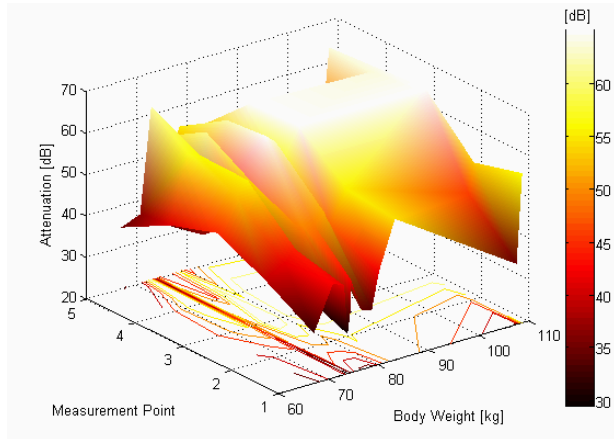


Figure 12: 3D representation of millimetre-wave Attenuation Versus Body Weight from Left-Right Torso

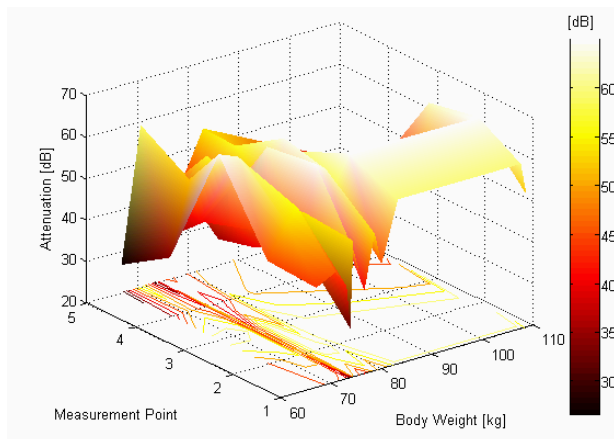


Figure 13: 3D representation of millimetre-wave Attenuation Versus Body Weights from Top-Bottom Torso

Figures 12 and 13 shows 3D representations of the combined data from figures 7 and 9, and figures 8 and 9 respectively. The data is flat for a region of body weights from 85 to 105 kg in Figures 12 and 13 due to a lack of measurement data (no subjects were studied with weights in this range).

The data presented in this paper will next be used together with a 3D ray tracing simulator to determine the impact of

people (individuals and crowds) at millimetre-wave frequencies in an indoor environment. Physical level solutions will then be explored to overcome these limitations.

5. CONCLUSION

A measurement campaign to determine the level of human body shadowing at 60 GHz was reported. This band is currently under investigation by the IEEE TG3c group for future wireless PANs. A simple linear relationship between the attenuation level observed, and the body weight, body fat and body water content of the subject was determined. From the anechoic chamber measurements, the average signal attenuation of the direct path through the torso was around 49 dB. Instantaneous attenuations varied between 34 dB to 65 dB depending on the individual and the part of the torso that was illuminated.

ACKNOWLEDGEMENTS

The authors are grateful to the University of Glamorgan, and in particular to Professor Miqdad Al-Nuaimi, for the supply of 60 GHz equipment. The support of Telmo R. Fernandes is gratefully acknowledged. The authors would also like to thank the Centre for Communications Research (University of Bristol), and their sponsors, for provision of laboratory facilities and use of its anechoic chamber.

REFERENCES

- [1] S. Obayashi, J. Zander, "A Body-Shadowing Model for Indoor Radio Communication Environments", *IEEE Transaction on Antennas and Propagation*, vol.46, no. 6, June 1998.
- [2] J. Hubber et al., "Simple channel model for 60 GHz indoor wireless LAN design based on complex wideband measurements," *Proceedings VTC '97*, vol.2, pp. 1004-1008, May 1997.
- [3] R. J. C. Bultitude, "Estimating frequency correlation functions from propagation measurements on fading radio channels: A critical review," *IEEE J. Sel. Areas Comm.* vol.20, no.6, pp. 1133-1143, Aug. 2002.
- [4] Sato, K.; Manabe, T, "Estimation of propagation-path visibility for indoor wireless LAN systems under shadowing condition by human bodies," *Vehicular Technology Conference*, vol.3, pp. 2109-2113, May 1998.
- [5] Moraitis, N.; Constantinou, P, "Indoor channel measurements and characterization at 60 GHz for wireless local area network applications," *IEEE Transactions on Antennas and Propagation*, vol.52, issue 12, pp. 3180-3189, Dec 2004.
- [6] Theodore Rappaport, "Wireless Communications: Principles and Practice," *Prentice Hall*, Oct 1995.